Visual Abstract

# Artificial neural network based delamination prediction in composite plates using vibration signals

T. G. Sreekanth, M. Senthilkumar, S. Manikanta Reddy
*Department of Production Engineering, PSG College of Technology, Coimbatore-641004, Tamilnadu, India.*
*sreekanthtg007@gmail.com, stg.prod@psgtech.ac.in, https://orcid.org/0000-0003-3848-7419*
*msk.prod@psgtech.ac.in, https://orcid.org/0000-0002-3720-0941*
*manikantaslv@gmail.com, https://orcid.org/0000-0003-3643-6052*

**ABSTRACT.** Dynamic loading on composite components may induce damages such as cracks, delaminations, etc. and development of an early damage detection technique for delamination prediction is one of the most important aspects in ensuring the integrity and safety of such components. The presence of damages such as delaminations on the composites reduces its stiffness and changes the dynamic behaviour of the structures. As the loss in stiffness leads to changes in the natural frequencies, mode shapes, and other aspects of the structure, vibration analysis may be the ideal technique for delamination prediction. In this research work, the supervised feed-forward multilayer back-propagation Artificial Neural Network is used to determine the position and area of delaminations in glass fiber-reinforced polymer (GFRP) plates using changes in natural frequencies as inputs. The natural frequencies were obtained by finite element analysis and results are validated experimentally. The findings show that the suggested technique can satisfactorily estimate the location and extent of delaminations in composite plates.

**KEYWORDS.** Health Monitoring, Composite, GFRP, Delamination, Vibration, natural frequency, Artificial Neural Network.

OPEN ACCESS

**Citation:** Sreekanth, T. G., Senthilkumar, M., Reddy, S. M., Artificial neural network based delamination prediction in composite plates using vibration signals, Frattura ed Integrità Strutturale, 63 (2023) 37-45.

**Received:** 05.09.2022
**Accepted:** 15.10.2022
**Online first:** 17.10.2022
**Published:** 01.01.2023



## INTRODUCTION

Composite materials have been trending in modern engineering designs over the last three decades as a result of their appealing mechanical qualities, stable physical and chemical characteristics, etc. These composites, on the other hand, are prone to failure mechanisms that are unique from those of metallic alloys [1]. There is growing concern about the maintenance of composite components as each non-destructive testing method has technical constraints in terms of size, material composition, and damage/failure modes of Fibre Reinforced Plastics (e.g. weak bond, matrix cracking, delamination and fibre cracking) [2].

Glass fiber-reinforced plastics and carbon fiber-reinforced plastics have become popular in present engineering applications and it is expected that this practice will continue in the future also [3]. E-glass laminates have become more common in aviation components such as wings, fuselages, and stabilisers; as stronger, more durable, and tougher resins

such as epoxies have evolved [4]. When the plane flies at a higher altitude, the trapped moisture/water expands, causing micro-cracking or delaminations. Furthermore, as time passes, aircraft may experience more flight cycles, and this process of freezing and unfreezing will cause micro-cracks to get larger, eventually leading to delaminations.
Delaminations can be caused by a flaw in the manufacturing, assembly, or in-service stages, or by a combination of these. Material/structural discontinuities that cause inter-laminar strains are the most common cause of delaminations [5]. Delaminations can also develop at stress-free edges due to mismatches in individual layer properties. It can also happen in areas where there is out-of-plane loading, such as when curved beams bend. Delaminations have a substantial impact on the composites' static and dynamic performance [6]. It is also an important type of failure in composites as delamination diminishes the composite's strength. When static loading is applied, there is a risk of local buckling when compression loading is applied. When this local buckling spreads to a relatively big delaminated part, the overall structure may break suddenly. Delamination reduces stiffness under dynamic stress, which might result in a larger deflection magnitude for the total structure. Foreign object impact is also a common cause of fibre reinforced polymer delaminations [7].
The vibration approach is a global damage detection method in which changes in physical parameters such as mass, damping, and stiffness cause changes in modal variables to be recognised. For damage diagnosis and quantification, the frequency-domain method employs changes in modal properties such as natural frequency, frequency response functions, damping, and mode shapes [8]. There is a requirement for finding natural frequency variations due to delamination generation in the method of delamination diagnosis in composite plates by vibration method, which can be produced using Finite Element Analysis. The composite type utilized for this study was glass fiber-reinforced polymer (GFRP). The inverse problem is used to determine the position and magnitude of delaminations in composite plates using changes in the first five natural frequencies as input. The methodology followed is shown in Fig. 1.

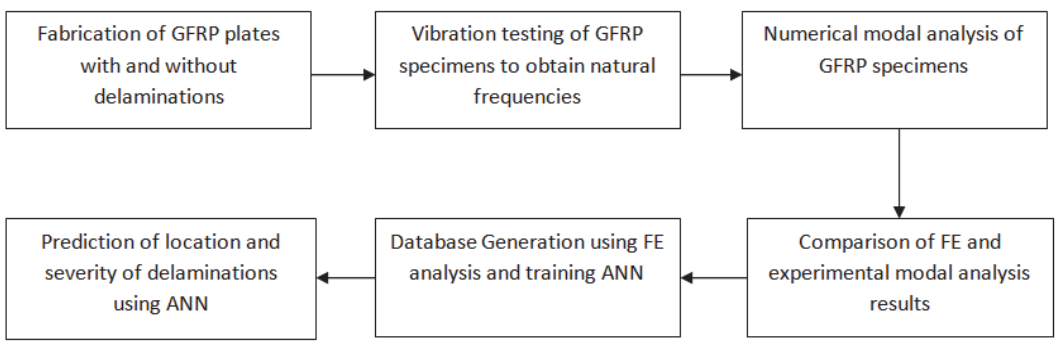


Figure 1: Methodology.

An analytical model is necessary to solve an inverse problem, which necessitates considerable effort in developing a mathematical framework that is both accurate and reliable. Artificial Neural Network (ANN) approaches can be applied to damage assessment techniques to overcome the complexity of framing mathematical frameworks [9, 10]. ANN is used to anticipate damage features since neural networks are now being used as universal function approximators for difficult problems. The desire to develop a good data pattern recognition and decision-making system has driven this research. The ANN was trained using a learning procedure that depicted the relationship between various inputs (here, the first five natural frequencies) and outputs (location and area of delaminations in plate).

## FABRICATION OF GFRP PLATES

The fabrication procedure was performed by hand layup. Glass fibre, epoxy resin, and hardener are used for the fabrication. There are 16 layers in the composite and the stacking sequence of $[0/45/-45/90]_{2S}$ was considered for the work. The glass fibre is cut from a roll of glass fibre with dimensions 250 mm × 250 mm. In a 10:1 ratio, epoxy resin and hardener are mixed. To shield the working table from resin spillage and easy removal of composite, a layer of polythene is laid over it. Over the polythene sheet, the first layer of the bidirectional woven E-glass fibre is laid, and the resin is applied with a brush to the first layer. The second layer is layered on top of the first layer and squeezed with rollers, then resin is softly applied over the second layer, and the process is repeated until the last layer is completed. The fabrication progression is shown in the Fig. 2.

Figure 2: Fabrication of composite plates.

GFRP specimens without delamination was made initially and the specimens with delamination was fabricated thereafter with a delamination dimensions of 40 mm x 40 mm, 40 mm x 60 mm, and 40 mm x 50 mm, for specimen 2, 3 and 4 respectively. There is no delamination in Specimen 1. For the specimen 2, delamination is created at seventh layer (50 mm x 50 mm away from the top right end), for specimen 3, delamination is created at fifth layer (100 mm x 100 mm away from the top right end) and for the specimen 4, delamination is created at ninth layer (150 mm x 150 mm away from the top right end). The delamination is made with Teflon tapes. Teflon tape was cut to the proportions of the delamination and put in the fibre laminates interface layers. After manufacturing, the GFRP was left to cure. At the carpentry shop, GFRPs were cut to 220 mm × 200 mm dimensions using a power tool machine. Extra 20 mm is given at one side for clamping purposes. Fabricated plate samples are shown in Fig. 3.

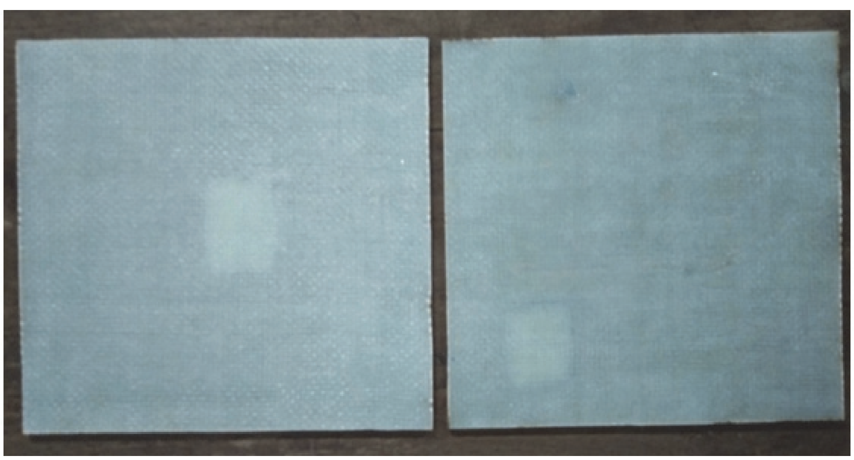

Figure 3: Fabricated GFRP plates.

## Vibration testing

The vibration testing experimental setup is shown in Fig. 4. The data acquisition system (DAQ), impact hammer, triaxial accelerometer, and computer with LabVIEW software comprise up the experimental setup. Cantilever clamping is used to hold the specimens. The effective dimensions of specimens after clamping are 220 mm × 200 mm. An impact hammer was used to excite the clamping plate, which applied an impulse force to the composite plate. Tri-axial accelerometer was used to capture the dynamic behaviour of the excited plate. The accelerometer was fixed in a way that z axis was pointing upwards and it is attached to the surface with petro wax adhesive. The accelerometer was attached to a data acquisition system, which amplified and translated the analogue signals provided by the accelerometer to digital signals. The DAQ was attached to the PC and LabVIEW software was used to interface with it.

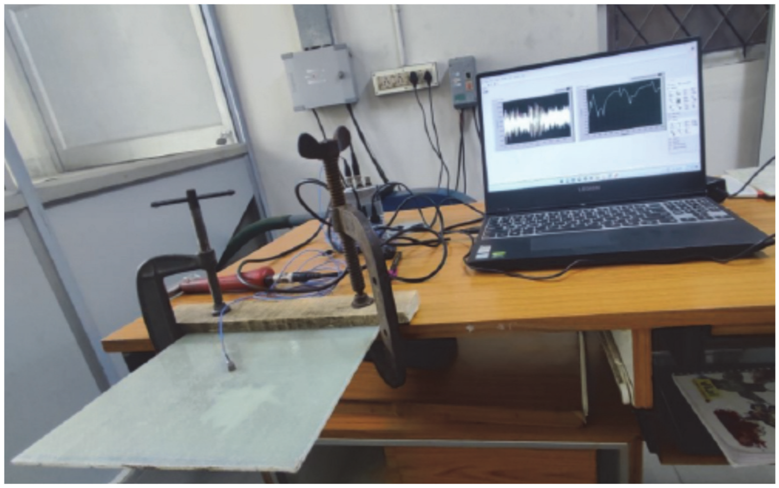

Figure 4: Experimental setup of vibration testing.

## Finite Element Analysis

Modal analysis is a way for investigating the dynamic features of a structure when it is vibrated. Modal analysis can be used to determine a structure's natural frequencies and mode shapes. Because modeling composite plates falls under the category of three-dimensional modeling of solid structures, the element type employed to simulate the plates was layered Solid 185. The number of elements examined for each layer along the thickness was one, and information about each layer is defined by shell element. First five natural frequencies are considered for this research work.

The natural frequencies were compared to the experimental data for undamaged and delaminated composite plates to validate the Finite Element Analysis (FEA) results. When the percentage error for each case is determined and compared, plates with and without delaminations have a maximum inaccuracy of 7 %. The differences in results could be due to inaccuracies in specimen production and faults in frequency measurement from vibration tests.

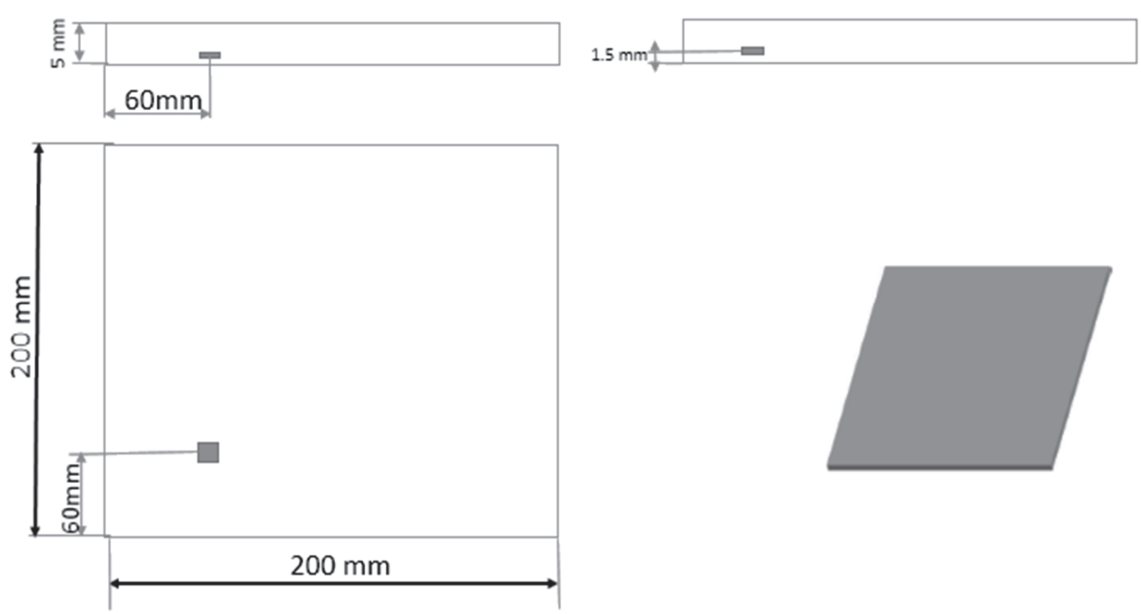


Figure 5: Sample delamination scenario.

| Coordinates (mm) X axis (mm) | Y axis (mm) | Z axis (mm) | Delamination Size ($mm^2$) | NF 1 (Hz) | NF 2 (Hz) | NF 3 (Hz) | NF 4 (Hz) | NF 5 (Hz) |
|---|---|---|---|---|---|---|---|---|
| X= 60 | Y=60 | Z=0.6 | 25 | 258.5 | 814.45 | 867.58 | 1849.3 | 1894.2 |
| X= 60 | Y=60 | Z=0.6 | 50 | 254.46 | 810.39 | 863.57 | 1839.9 | 1889.3 |
| X= 60 | Y=60 | Z=0.6 | 75 | 250.41 | 806.37 | 859.51 | 1834.7 | 1884.2 |
| X= 60 | Y=60 | Z=0.6 | 100 | 246.26 | 802.28 | 855.48 | 1831.2 | 1879.6 |
| X= 60 | Y=60 | Z=0.6 | 125 | 241.85 | 798.13 | 851.48 | 18519.6 | 1874.1 |
| X= 60 | Y=60 | Z=1.5 | 25 | 256.49 | 812.42 | 865.15 | 1847.1 | 1892.6 |
| X= 60 | Y=60 | Z=1.5 | 50 | 254.4 | 809.6 | 862.2 | 1839.2 | 1879.9 |
| X= 60 | Y=60 | Z=1.5 | 75 | 250.32 | 805.26 | 858.16 | 1834.2 | 1874.5 |
| X= 60 | Y=60 | Z=1.5 | 100 | 245.26 | 800.84 | 853.1 | 1821.6 | 1870.2 |
| X= 60 | Y=60 | Z=1.5 | 125 | 240.25 | 796.25 | 848.48 | 1809.4 | 1859.6 |
| X= 60 | Y=60 | Z=2.40 | 25 | 256.3 | 812.24 | 865.01 | 1846.5 | 1892.5 |
| X= 60 | Y=60 | Z=2.40 | 50 | 253.8 | 810.21 | 862.15 | 1839.8 | 1878.9 |
| X= 60 | Y=60 | Z=2.40 | 75 | 249.22 | 803.84 | 858.14 | 1835.2 | 1873.5 |
| X= 60 | Y=60 | Z=2.40 | 100 | 245.2 | 799.4 | 847.9 | 1830.8 | 1868.2 |
| X= 60 | Y=60 | Z=2.40 | 125 | 240.9 | 794.54 | 843.47 | 1819.7 | 1860.6 |
| X= 60 | Y=60 | Z=3.3 | 25 | 256.25 | 812.22 | 865.62 | 1846.2 | 1892.6 |
| X= 60 | Y=60 | Z=3.3 | 50 | 254.16 | 810.26 | 863.54 | 1838.5 | 1890.12 |
| X= 60 | Y=60 | Z=3.3 | 75 | 249.24 | 805.46 | 859.25 | 1834.4 | 1885.6 |
| X= 60 | Y=60 | Z=3.3 | 100 | 245.12 | 801.03 | 855.05 | 1829.4 | 1881.2 |
| X= 60 | Y=60 | Z=3.3 | 125 | 241.1 | 796.95 | 850.47 | 1824.6 | 1877.6 |
| X= 60 | Y=60 | Z=4.1 | 25 | 256.12 | 812.2 | 865.25 | 1845.5 | 1892.1 |
| X= 60 | Y=60 | Z=4.1 | 50 | 253.24 | 809.46 | 863.14 | 1838.4 | 1889.92 |
| X= 60 | Y=60 | Z=4.1 | 75 | 249.16 | 805.03 | 858.25 | 1834.4 | 1885.6 |
| X= 60 | Y=60 | Z=4.1 | 100 | 245.1 | 800.95 | 854.05 | 1829.31 | 1881.15 |
| X= 60 | Y=60 | Z=4.1 | 125 | 241 | 795.69 | 849.47 | 1824.5 | 1876.6 |

Table 1: Dataset for the location X=60 mm Y=60 mm.

## DATABASE GENERATION

A database of shifts in frequencies (due to known delaminations) is required to train the inverse algorithm. With the aid of finite element analysis, the appropriate database is created. A significant number of composite plate samples with various sizes and locations of delaminations were subjected to numerical analysis. The database size required to train ANN is important for properly diagnosing delaminations. Two hundred and twenty five distinct delamination scenarios were created numerically for this study by combining delaminations at nine different places (combinations of x = 60, 120, 180; and Y = 60, 120, 180; where x and y are distance of delaminations location from bottom left end.), five different sizes (25, 50, 75, 100, 125 $mm^2$) and five different layers (Layer 2, 5, 8, 11 & 14).
Fig. 5 shows an example of one of the delaminations scenarios, with delaminations at x=60, y=60 and a delaminations area of 25 $mm^2$ on layer 5. Tab. 1 shows the first five natural frequencies of the plate sample with delaminations at X=60, Y=60, and Z=0.6, for five delamination areas. A similar dataset is created for the remaining eight locations. Fig. 6 (a) and (b) illustrate the bending modes for the same sample delaminated plate with delamination size of 25 $mm^2$.

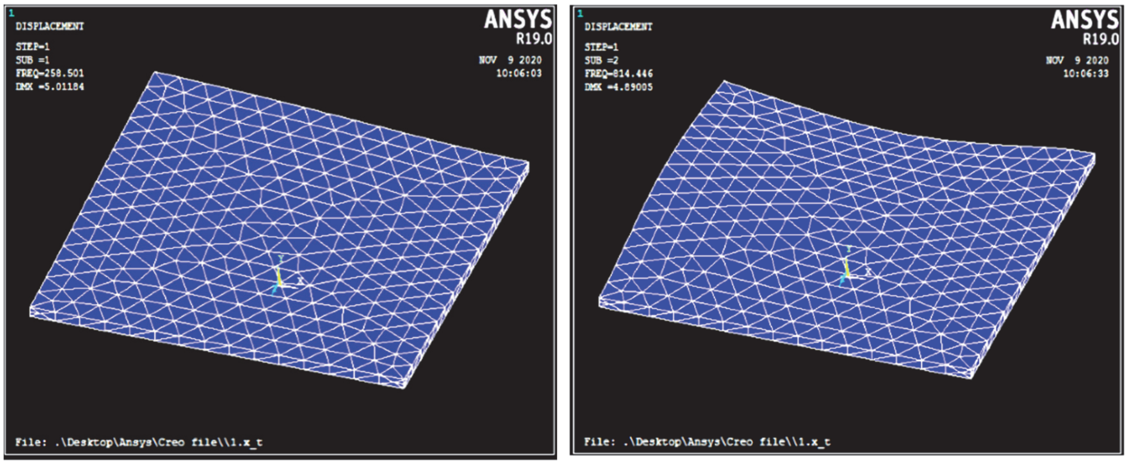


Figure 6: (a) Bending Mode 1, (b) Bending Mode 2.

## Feed-Forward Back-Propagation Neural Network

A neural network functions as a processor, storing and retrieving experience based information as and when needed. In terms of accumulating information through the learning process, it functions similarly to the human brain [11]. Learning is a process in which the parameters of a neural network, such as synaptic weights and bias levels, are modified in a continuous manner. The difference between a feed forward neural network and a recurrent neural network is that the connections between each unit do not form a loop. Furthermore, information only moves in one way, that is, forward, from the input nodes to the output nodes via the hidden nodes. As a result, no loops arise in this network.

There are two types of learning processes: supervised learning and unsupervised learning. The system will try to anticipate the results based on known samples dataset in supervised learning approach, which is also the most often used training technique [12]. It will compare its own predictions to known goal values, after which it will learn from the errors encountered throughout each cycle. The data will flow from the input layer to the neurons, which will then transfer the data to the next nodes. Weights and connections are given as data passes along, and when the data reaches the successor node, the weights are added and either weakened or intensified. There will be no changes to the weights if the output obtained is equivalent to the expected output [13-15]. However, if the output obtained differs from the real result, the error will propagate backwards through the system, and the weights will be adjusted accordingly. Back-propagation refers to the reverse flow of error through the neural network. Supervised feed-forward multilayer back-propagation Artificial Neural Network tool in MATLAB is used for this research based on findings from various literatures [16-17].

## Neural Network Training

To improve the model and verify the hypothesis, inverse techniques employ both the original model of the structure (here, a delaminated plate) and observed data (here, the first five natural frequencies). The goal here is to see how effective global vibration parameters (natural frequencies) as input to an ANN back-propagation algorithm are in locating and predicting the location and magnitude of delaminations. The ANN size is critical since smaller networks cannot correctly reflect the system, while bigger networks over-train it. As illustrated in Fig. 7, the ANN used here has five inputs (frequencies), four outputs (position in x and y directions, layer, and size of delamination), and one hidden layer with 12 neurons. All the parameters are optimized to get the maximum accuracy. The mean square error (MSE) is utilised as an ANN's performance metric, and the Levenberg-Marquardt back-propagation technique is employed to train it.

As discussed in database generation section, 225 input-output dataset is created and out of which 155 are used for training, 35 each used for testing and validation. Fig. 8 depicts the linear regression analysis of the target and anticipated values. The Pearson's correlation coefficients (R-values) for training, validating, testing, and total data are 0.908, 0.931, 0.912, and 0.912, respectively. This indicates that the ANN-based prediction model is providing a satisfactory match to the data.

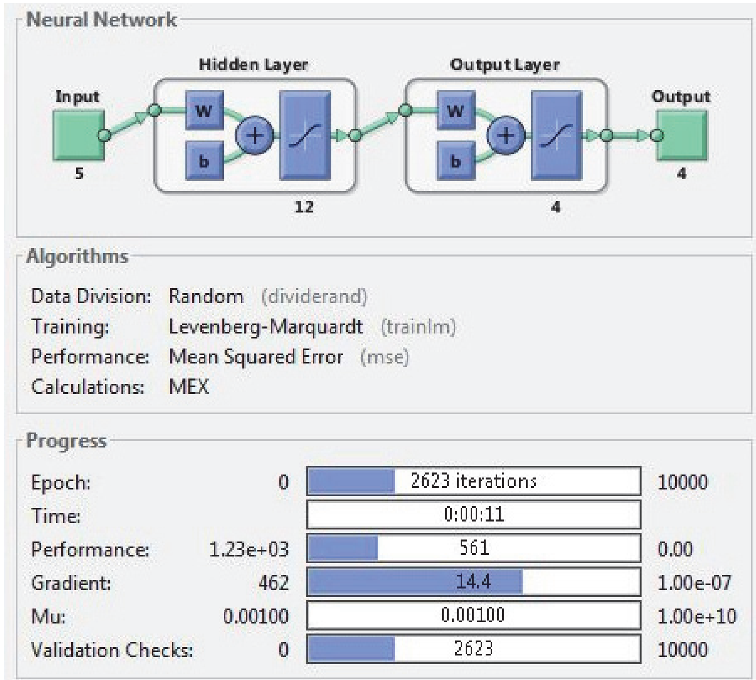


Figure 7: Neural Network used for Delamination Prediction.

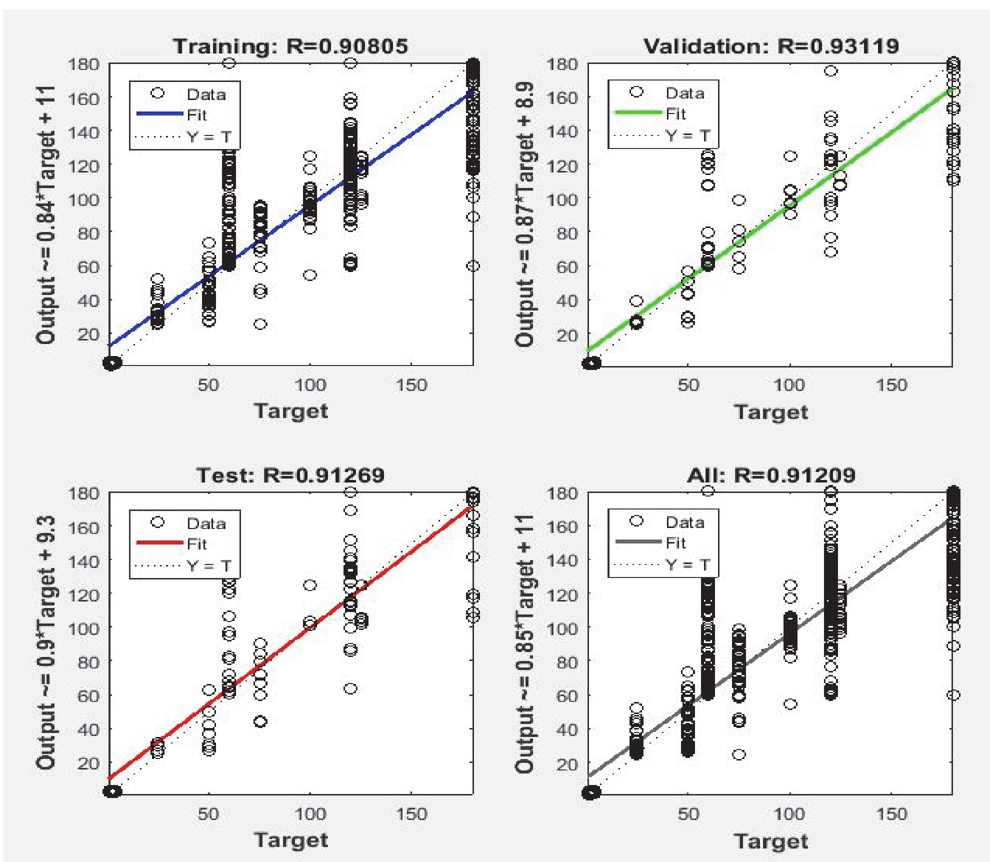


Figure 8: Regression Analyses of Data Predicted by the ANN Model.

## RESULTS FOR DELAMINATION PREDICTION

Five finite element models were created to test the ANN approach for determining delamination location and area in composite plates. Tab. 2 shows the actual and estimated values of layer, position, and delamination area. In the table, the real values of delaminations are assigned values that are chosen at random.

| | Plate Number | Actual | Predicted | Percentage Error |
|---|---|---|---|---|
| Delamination location – X (mm) | 1 | 50 | 58.2 | 16.4 |
| | 2 | 75 | 81.25 | 8.3 |
| | 3 | 100 | 93.6 | -6.4 |
| | 4 | 125 | 114 | -8.8 |
| | 5 | 150 | 164 | 9.3 |
| Delamination location – Y (mm) | 1 | 75 | 61.3 | -18.2 |
| | 2 | 100 | 80.5 | -19.5 |
| | 3 | 125 | 109 | -12.8 |
| | 4 | 150 | 121.2 | -19.2 |
| | 5 | 175 | 163.9 | -6.3 |
| Delamination location – Z (mm) | 1 | 0.9 | 0.73 | -18.9 |
| | 2 | 1.2 | 1.1 | -8.3 |
| | 3 | 1.8 | 1.76 | -2.2 |
| | 4 | 2.1 | 2.23 | 6.2 |
| | 5 | 3 | 2.87 | -4.3 |
| Delamination Area ($mm^2$) | 1 | 30 | 27.6 | -8.0 |
| | 2 | 60 | 61.5 | 2.5 |
| | 3 | 90 | 93.5 | 3.9 |
| | 4 | 110 | 104.6 | -4.9 |
| | 5 | 140 | 121.2 | -13.4 |

Table 2: Comparison of Actual and Predicted Delamination Parameters for Composite Plates

When compared to findings for y direction location, the values for delaminations area, position in x direction, and layer prediction were better for all 5 plate samples. Plate 1 seemed to have the highest x axis location prediction error of 16.4 percent, but it was the only example where the x axis location error above 10%. The reason for this error is may be because of the reason that actual location was out of the training dataset. For y direction prediction, it can be understood that all plates except plate 5 have error greater than 10%. Layer prediction inaccuracy was within 10% for all plates, except for plate 1. Error in delamination area forecast for plate 5 alone crossed 8%. The reason for this case may be that, the actual area was outside the training data considered. The reason for overall error may be because of more complexity in plate delaminations prediction because of more number of inputs (four) to the neural network. It's also worth noting that the inaccuracy was particularly significant when predictions were made outside of the training dataset. This indicates that the findings can be further improved by expanding the training dataset.

## CONCLUSIONS

Vibration-based analysis on composite plates is offered in this study effort to forecast the severity and location of the delamination. After confirming with experiments, numerical models of non-delaminated and delaminated composite plates were built, and the first five natural frequencies for various delamination situations were produced. Natural frequencies are degraded by delamination in composite plates, according to research. These findings were utilised to train the neural network, which was then used to create the inverse algorithms. The first five natural frequencies are fed into the ANN, which then takes outputs as delamination scenarios. Numerical frequency data was used to track the neural network's performance in evaluating delaminations. It was observed that the ANN was able to estimate the delaminations in composite plates with reasonably good precision. Neural networks have a lot of benefits, such as the need for less statistical training, the capacity to recognise intricate nonlinear correlations among variables, the capacity to recognise all potential interactions among predictor variables, etc. An increased computing overhead, tendency for overfitting, and the empirical nature of model development are drawbacks for neural networks.

## REFERENCES

[1] Senthilkumar, M., Sreekanth, T. G. and Reddy, S. M. (2020) Nondestructive health monitoring techniques for composite materials: A review. Polym Polym Compos 29, 528-540. DOI: 10.1177/0967391120921701

[2] Onggar, T., Häntzsche, E., Hund, R.D. and Chokri, C (2019) Multilayered Glass Filament Yarn Surfaces as Sensor Yarn for In-situ Monitoring of Textile-reinforced Thermoplastic Composites. Fibers Polym 20, 1945–1957. DOI: 10.1007/s12221-019-1237-2

[3] Zhou, W., Wei, Zy., Wang, Gf., Han, Kn., Liu, R. and Ma, Lh. (2021) Transverse Tensile Deformation and Failure of Three-dimensional Five-directional Braided Carbon Fiber Composites. Fibers Polym 22, 1099–1110. DOI: 10.1007/s12221-021-9199-6

[4] Sreekanth, T.G., Senthilkumar, M. and Reddy, S.M. (2021) Vibration-based delamination evaluation in GFRP composite beams using ANN. Polym Polym Compos 29, 317-324. DOI: 10.1177/09673911211003399

[5] Kindova-Petrova, D. (2014) Vibration-based methods for detecting a crack in a simply supported beam, J. Theor. Appl. Mech. 44, 69–82. DOI: 10.2478/jtam-2014-0023

[6] Sreekanth, T.G., Senthilkumar, M. and Reddy, S.M. (2021) Fatigue Life Evaluation of Delaminated GFRP Laminates Using Artificial Neural Networks. Trans Indian Inst Met 74, 1439–1445. DOI: 10.1007/s12666-021-02234-5

[7] Liu, Y.J., Jiang, Z., Wen, H.M. (2020) Predicting impact induced delamination of FRP laminates. Int. J. Impact Eng.. DOI: 10.1016/j.ijimpeng.2019.103436

[8] Senthilkumar, M., Reddy, S. M. and Sreekanth, T.G. (2022) Dynamic Study and Detection of Edge Crack in Composite Laminates Using Vibration Parameters. Trans Indian Inst Met 75, 361–370. DOI: 10.1007/s12666-021-02419-y

[9] Pagani, A., Enea, M., Carrera, E. (2021) Component-wise damage detection by neural networks and refined FEs training. J. Sound Vib. DOI: 10.1016/j.jsv.2021.116255

[10] Sreekanth, T.G., Senthilkumar, M. and Reddy, S.M. (2022) Natural Frequency based delamination estimation in GFRP beams using RSM and ANN. Frattura ed Integrità Strutturale 61, 487-495. DOI: 10.3221/IGF-ESIS.61.32

[11] Bilisik, K., Demiryurek, O. (2011) Analysis and tensile-tear properties of abraded denim fabrics depending on pattern relations using statistical and artificial neural network models. Fibers Polym 12, 422. DOI: 10.1007/s12221-011-0422-8

[12] Ribeiro, J.P., Tavares, S.M., Parente, M. (2021) Stress–strain evaluation of structural parts using artificial neural networks. Proc. Inst. Mech. Eng. L P I MECH ENG L-J MAT. DOI: 10.1177%2F1464420721992445

[13] Aadatmorad, M., Talookolaei, R. A.-J., Pashaei, M.-H., Khatir, S. and Wahab, M.A. (2022). Pearson Correlation and Discrete Wavelet Transform for Crack Identification in Steel Beams, Mathematics 10, 2689. DOI: 10.3390/math10152689

[14] Zenzen, R., Khatir, S., Belaidi, I., Le Thanh, C., Wahab, M. A. (2020) A modified transmissibility indicator and Artificial Neural Network for damage identification and quantification in laminated composite structures, Composite Structures 248, 112497, DOI: 10.1016/j.compstruct.2020.112497.

[15] Khatir, S., Tiachacht, S., Le Thanh, C., Ghandourah, E., Mirjalili, S., Wahab, M. A. (2021) An improved Artificial Neural Network using Arithmetic Optimization Algorithm for damage assessment in FGM composite plates, Composite Structures 273, 114287, DOI: 10.1016/j.compstruct.2021.114287.

[16] Al Thobiani, F., Khatir, S., Benaissa, B., Ghandourah, E., Mirjalili, S. and Wahab, M. A. (2022) A hybrid PSO and Grey Wolf Optimization algorithm for static and dynamic crack identification, Theoretical and Applied Fracture Mechanics 118, 103213, DOI: 10.1016/j.tafmec.2021.103213.